

Journal of Biomedical Optics

BiomedicalOptics.SPIEDigitalLibrary.org

Comparative evaluation of methylene blue and demeclocycline for enhancing optical contrast of gliomas in optical images

Dennis Wirth
Matija Snuderl
William Curry
Anna Yaroslavsky

Comparative evaluation of methylene blue and demeclocycline for enhancing optical contrast of gliomas in optical images

Dennis Wirth,^a Matija Snuderl,^b William Curry,^c and Anna Yaroslavsky^{a,*}

^aUniversity of Massachusetts Lowell, Department of Physics and Applied Physics, One University Avenue, Lowell, Massachusetts 01854, United States

^bNYU Langone Medical Center and Medical School, Department of Pathology, 530 First Avenue, Tisch 480, New York, New York 10016, United States

^cMassachusetts General Hospital, Department of Neurosurgery, Harvard Medical School, 55 Fruit Street, Gray 502, Boston, Massachusetts 02114, United States

Abstract. Contrast agents have shown to be useful in the detection of cancers. The goal of this study was to compare enhancement of brain cancer contrast using reflectance and fluorescence confocal imaging of two fluorophores, methylene blue (MB) and demeclocycline (DMN). MB absorbs light in the red spectral range and fluoresces in the near-infrared. It is safe for *in vivo* staining of human skin and breast tissue. However, its safety for staining human brain is questionable. Thus, DMN, which absorbs light in the violet spectral range and fluoresces between 470 and 570 nm, could provide a safer alternative to MB. Fresh human gliomas, obtained from surgeries, were cut in half and stained with aqueous solutions of MB and DMN, respectively. Stained tissues were imaged using multimodal confocal microscopy. Resulting reflectance and fluorescence optical images were compared with hematoxylin and eosin histopathology, processed from each imaged tissue. Results indicate that images of tissues stained with either stain exhibit comparable contrast and resolution of morphological detail. Further studies are required to establish the safety and efficacy of these contrast agents for use in human brain. © The Authors. Published by SPIE under a Creative Commons Attribution 3.0 Unported License. Distribution or reproduction of this work in whole or in part requires full attribution of the original publication, including its DOI. [DOI: [10.1117/1.JBO.19.9.090504](https://doi.org/10.1117/1.JBO.19.9.090504)]

Keywords: glioblastoma; methylene blue; demeclocycline; reflectance; fluorescence; confocal imaging.

Paper 140338LR received Jun. 2, 2014; revised manuscript received Aug. 11, 2014; accepted for publication Aug. 18, 2014; published online Sep. 19, 2014.

1 Introduction

Brain tumors are the seventh most common form of human cancers. Gliomas constitute 80% of primary brain malignancies.¹ In

contrast to the solid central component, infiltrative portions of gliomas are often difficult to delineate using standard radiologic modalities due to lack of neovascularization, limited changes to pre-existent vessels, and comparatively low (approximately millimeter) resolution. Evidence suggests that more extensive resection combined with neurocognitive function preservation is associated with longer life expectancy and better quality of life.² The goal of this study was to determine the feasibility of using contrast agents for intraoperative high-resolution delineation of brain cancers to facilitate maximal resection of brain cancer tissue. We have shown that reflectance and fluorescence confocal imaging of methylene blue (MB) stained brain tissue was capable of delineating neoplasms *ex vivo*.^{3,4} However, clinical observations suggest the possibility of adverse neurologic effects after MB injection in the central nervous system.⁵ To address this issue, we have tested an antibiotic of the tetracycline family, demeclocycline (DMN), for detecting gliomas and compared the images with those obtained using MB stain. Antibiotics of the tetracycline family are commonly used to treat infection and inflammatory disorders. In addition, these fluorophores have affinity to cancer cells.^{6–8} To confirm the suitability of DMN for delineating brain cancers, we collected fresh brain tumor tissues, stained the samples with MB or DMN, acquired optical images, and compared them to each other and to corresponding histopathology.

2 Materials and Methods

All experiments were performed under approved IRB protocols of Massachusetts General Hospital (MGH) and University of Massachusetts Lowell (UML). Gliomas were collected from surgeries performed at MGH and delivered to the UML for imaging within 1 to 12 h of surgery. Time variation did not interfere with the quality of imaging and there were no significant changes of the brain tissue optical properties.⁹ Samples ranged in size between 2 and 40 mm³. Upon arrival to UML, each sample was vertically bisected along the short axis of the specimen into two halves. One half of the sample was placed in 0.05 mg/ml Dulbecco's phosphate buffered saline (DPBS, Mediatech Inc., Manassas, Virginia, USA) solution of MB (methylene blue injection, 1% American Regent Inc., Shirley, New York, USA), and the other half was placed in 1 mg/ml DPBS solution of DMN. After staining, samples were rinsed of excessive dye, mounted in a sample holder, and imaged. After imaging, tissues were fixed in 10% formalin (Ricca Chemical, Arlington, Texas, USA) and processed for paraffin-embedded hematoxylin and eosin (H&E) histopathology.

Confocal imaging of samples stained in MB was done as described elsewhere.^{3,4} For confocal imaging of DMN-stained samples, the imaging system was modified to allow for the excitation of DMN and detection of DMN fluorescence signal. In particular, a 402-nm diode laser (MicroLaser Systems, Garden Grove, California, USA) was used as the light source. All optical elements were selected to optimize the efficiency of light propagation in the visible spectral range. DMN fluorescence was separated with a dichroic mirror (Chroma, Bellows Falls, Vermont, USA), which reflected wavelengths >420 nm, and focused by a lens onto a 100- μ m pinhole placed in front of the fluorescence photomultiplier tube (PMT). A 520-nm band-pass filter with an FWHM of 40 nm (Edmund Optics, Barrington, New Jersey, USA) was utilized for DMN fluorescence imaging. Elastically scattered light was deflected by a nonpolarizing beam splitter (MellesGriot, Albuquerque, New Mexico, USA) and focused

*Address all correspondence to: Anna Yaroslavsky, E-mail: Anna_Yaroslavsky@uml.edu

onto a 100- μm pinhole in front of the reflectance PMT. We employed a 60 \times /1.2 NA water-immersion objective lens (Olympus, Melville, New Jersey, USA), which provided a 250- μm field of view, lateral resolution of better than 0.9 μm , and axial resolution of 2.5 μm . Power incident on the samples did not exceed 1.3 mW.

After imaging, H&E paraffin-embedded histopathology was processed and digitized as described elsewhere.^{3,4}

3 Results

In total, we imaged seven glioblastoma (GBM) specimens. GBMs are grade IV gliomas characterized by high cellularity, nuclear pleomorphism, microvascular proliferation, and necrosis. These tumors are among the most aggressive human cancers. All imaged samples showed histological features that were consistent with a high-grade glioma. Example reflectance and fluorescence images of a typical GBM are presented in Figs. 1(a) and 1(b), respectively. Comparison of the features in the images of Figs. 1(a) and 1(b) to histopathology, presented in Fig. 1(c), demonstrates that reflectance images emphasize highly scattering connective tissue of blood vessels (dashed arrows), whereas fluorescence images highlight cancer cells (solid arrows). Higher-magnification images of another glioma specimen are presented in Fig. 2. Comparison of both reflectance [Fig. 2(a)] and fluorescence [Fig. 2(b)] images to histopathology [Fig. 2(c)] demonstrate good correlation. Interestingly, reflectance image shows disrupted cell processes (dotted arrows), which, due to tissue processing, cannot be easily identified in histopathology. Similar to the image in Fig. 1(b), tumor cells in the fluorescence image [Fig. 2(b)] exhibit high contrast.

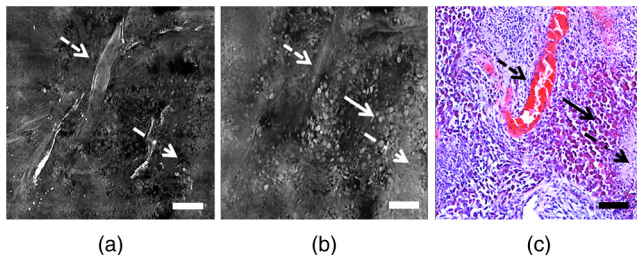


Fig. 1 Images of glioblastoma (GBM). Scale bar = 100 μm . (a) 402 nm reflectance image. (b) demeclocycline (DMN) fluorescence image. (c) H&E histopathology image. Solid arrows point to tumor cells, dashed arrows point to blood vessels, and dash and dotted arrows point to necrosis.

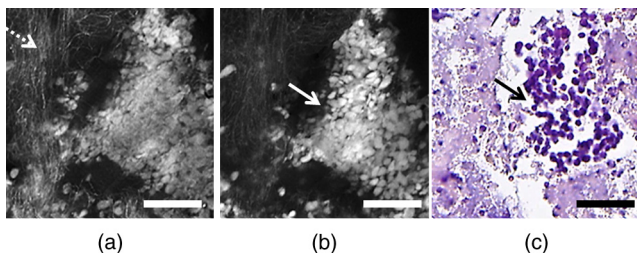


Fig. 2 Images of GBM. Scale bar = 100 μm . (a) 402 nm reflectance image. (b) DMN fluorescence image. (c) H&E histopathology image. Solid arrows point to tumor cells and dotted arrows point to tissue processes.

Our previous study³ showed that gliomas, stained with MB, provide high contrast between healthy and neoplastic tissue. Pathologists and neuropathologists, in particular, were successful in differentiating primary brain tumors from metastases and meningioma.⁴

To compare DMN and MB staining, in Fig. 3, we show images of the two halves of a GBM sample, stained with DMN and MB. Reflectance images of DMN- and MB-stained parts of GBM are shown in Figs. 3(a) and 3(b), respectively. Comparison of the reflectance image of DMN-stained tissue with histopathology [Fig. 3(c)] demonstrates high contrast of a blood vessel (dashed arrow). Blood vessel wall is bright, due to high scattering of connective tissue, whereas tumor cells exhibit comparatively low contrast (solid arrows), since the 402 nm wavelength is on the tail of the DMN absorption band, which has a maximum at 375 nm. In contrast, MB-stained tumor cells [solid arrow in Fig. 3(b)] exhibit higher contrast, since 642 nm corresponds to the maximum of MB absorption. Similarly, blood vessel appears dark due to MB uptake by endothelial cells and lower, as compared to 402 nm, scattering of the connective tissue. Fluorescence images of DMN- and MB-stained parts of GBM are presented in Figs. 3(d) and 3(e), respectively. Both fluorescence images highlight GBM tumor cells (solid arrows) and endothelial cells (dashed arrows). Comparison of the images in Figs. 3(d) and 3(e) demonstrate similar contrast and dye localization pattern.

To quantify the contrast enhancement, yielded by DMN and MB, for images in Fig. 3, we calculated the normalized average pixel values (NAPV_s) given by the following equation: $\text{NAPV}_s = \text{APV}_s / \text{APV}_i$, where APV_s is the mean of the pixel value exhibited by the structure and APV_i is the average pixel value of the entire image. In particular, we have analyzed the contrast of blood vessel and tumor cells. The results, summarized in Fig. 4, confirm our qualitative assessment of images in Figs. 1 and 2 and demonstrate that the contrast achieved in the

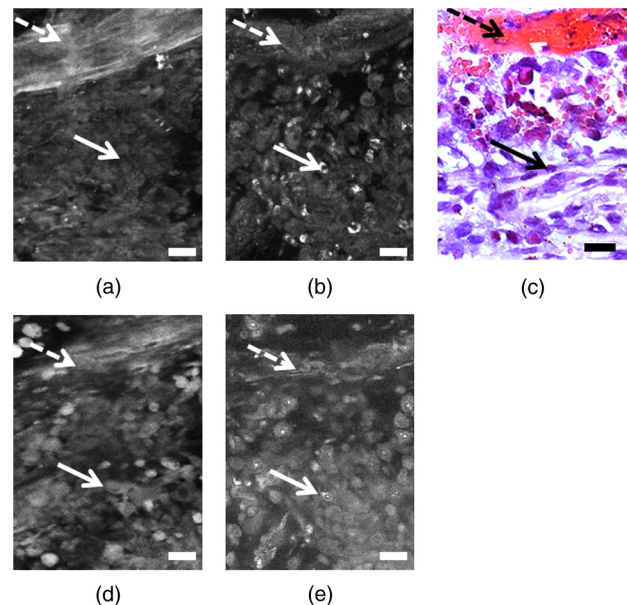


Fig. 3 Images of GBM. Scale bar = 100 μm . (a) 402 nm reflectance image. (b) 642 nm reflectance image. (c) H&E histopathology. (d) DMN fluorescence image. (e) Methylene blue fluorescence image. Solid arrows point to the tumor cells and dashed arrows point to blood vessels.

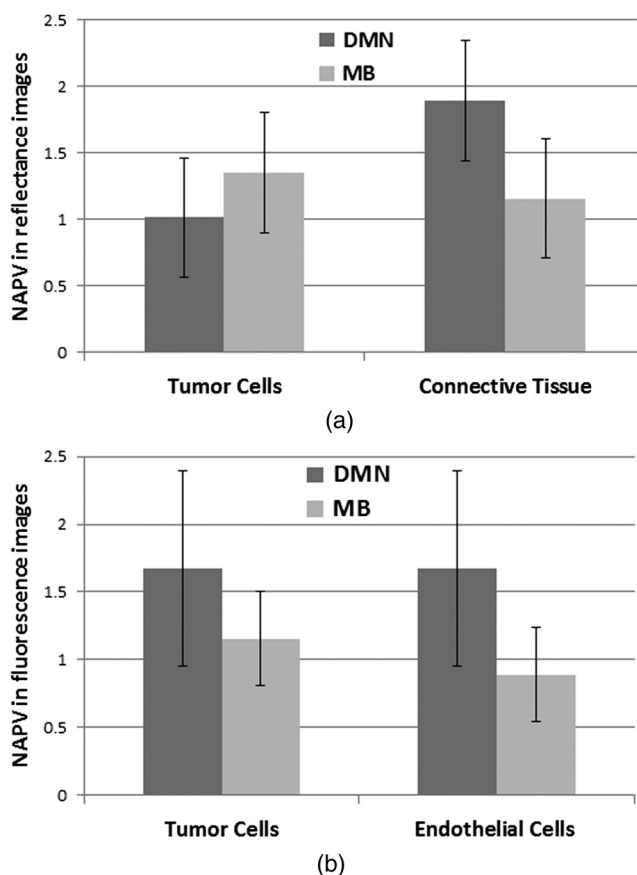


Fig. 4 (a) Normalized average pixel values (NAPV) of the tumor cells and connective tissue in the reflectance images of Figs. 3(a) and 3(b). (b) NAPV of the tumor cells (averaged over 40 cells) and endothelial cells in the blood vessel (averaged over seven cells) calculated from the fluorescence images of Figs. 3(d) and 3(e).

optical images of DMN-stained tissue is similar to that in the MB-stained tissue.

In summary, the results of our study indicate that optical images of tissues stained with MB and DMN exhibit similar staining patterns, contrast enhancement, and display good correlation with histopathology. Similar to MB, DMN emphasizes diagnostic features that enable interpretation of optical images in

a manner similar to H&E histopathology. In this feasibility study, following reported protocols for imaging DMN-stained skin tissue,^{8,10} we chose DMN concentration of 1 mg/ml for topical staining. However, since literature indicates that tetracycline derivatives are retained in cancer,^{6,11} DMN can be administered to patients orally for *in vivo* imaging. Therefore, future clinical efforts will focus on determining concentrations required for imaging *in vivo* brain tissue. Future studies will also focus on imaging other types of brain cancer and determining sensitivity and specificity of diagnosing optical images by neuropathologists.

Acknowledgments

We acknowledge I. Tabatadze for processing histopathology and C. Kwon for sample transportations. Funding was provided by MGH Cancer Center and UML seed grant.

References

1. "Brain and spinal cord tumors in adults," March 5, 2014, <http://www.cancer.org/acs/groups/cid/documents/webcontent/003088-pdf.pdf> (1 May 2014).
2. N. Sanai and M. Berger, "Glioma extent of resection and its impact on patient outcome," *Neurosurgery* **62**(4), 753 (2008).
3. D. Wirth et al., "Identifying brain neoplasms using dye-enhanced multimodal confocal imaging," *J. Biomed. Opt.* **17**(2), 026012 (2012).
4. M. Snuderl et al., "Dye-enhanced multimodal confocal imaging as a novel approach to intraoperative diagnosis of brain tumors," *Brain Pathol.* **23**(1), 73–81 (2013).
5. L. Vutskits et al., "Adverse effects of methylene blue on the central nervous system," *Anesthesiology* **108**(4), 684–692 (2008).
6. D. Rall et al., "Appearance and persistence of fluorescent material in tumor tissue after tetracycline administration," *J. Natl. Cancer Inst.* **19**(1), 79–85 (1957).
7. B. Holman et al., "Tumor detection and localization with Tc99m-tetracycline," *Radiology* **112**(1), 147–153 (1974).
8. Z. Tannous et al., "Delineating melanoma using multimodal polarized light imaging," *Laser Surg. Med.* **41**(1), 10–16 (2009).
9. A. N. Yaroslavsky et al., "Optical properties of selected native and coagulated human brain tissues *in vitro* in the visible and near infrared spectra range," *Phys. Med. Biol.* **47**(12), 2059–2073 (2002).
10. A. N. Yaroslavsky et al., "Fluorescence polarization of tetracycline derivatives as a technique for mapping nonmelanoma skin cancers," *J. Biomed. Opt.* **12**(1), 014005 (2007).
11. J. R. McLeary, "The use of systematic tetracyclines and ultraviolet in cancer detection," *Am. J. Surg.* **96**(3), 415–419 (1958).